# Supplemental Figures

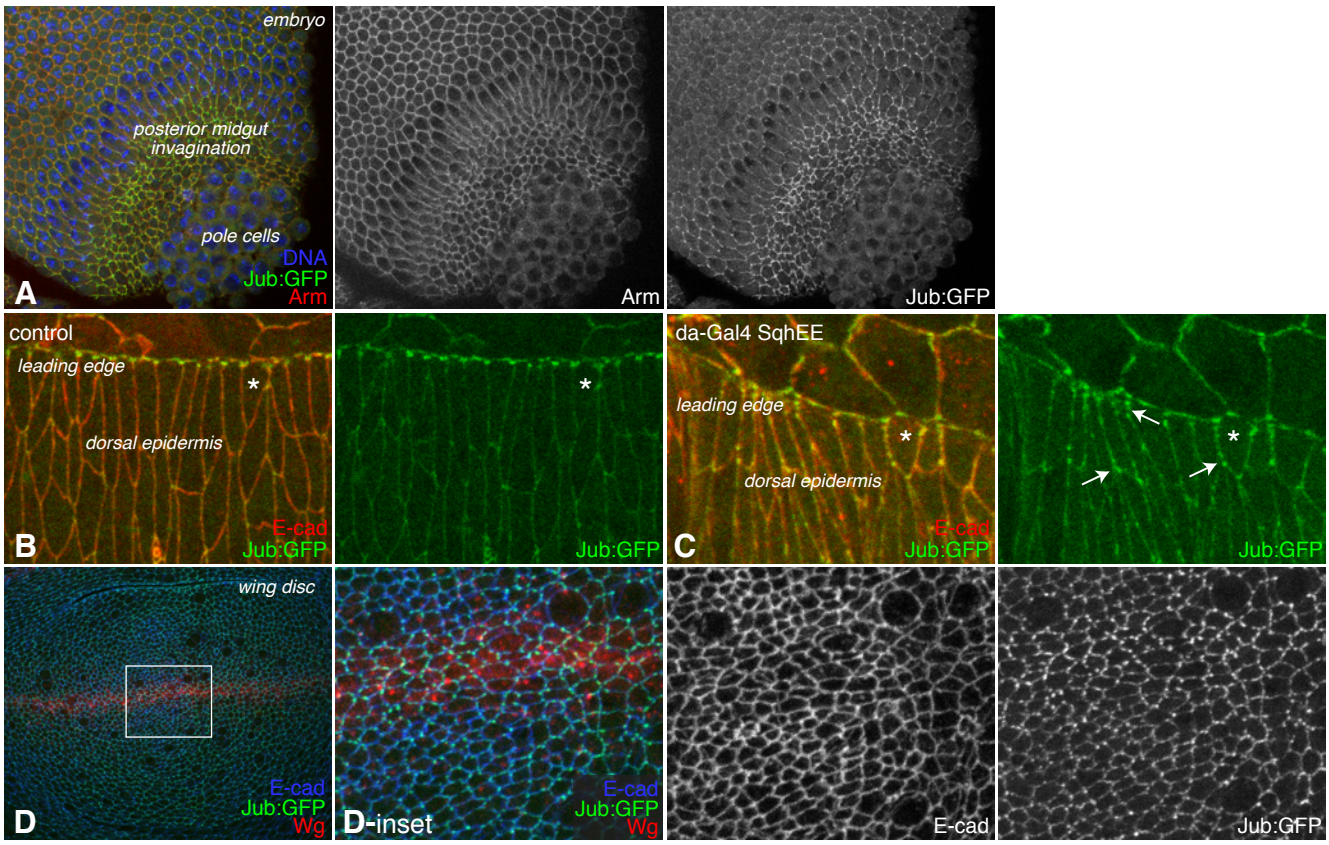


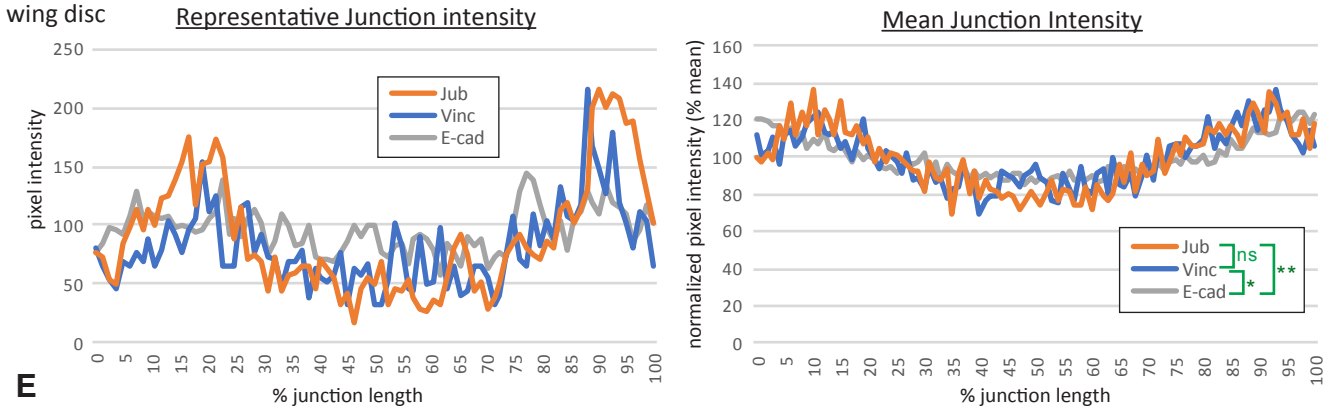


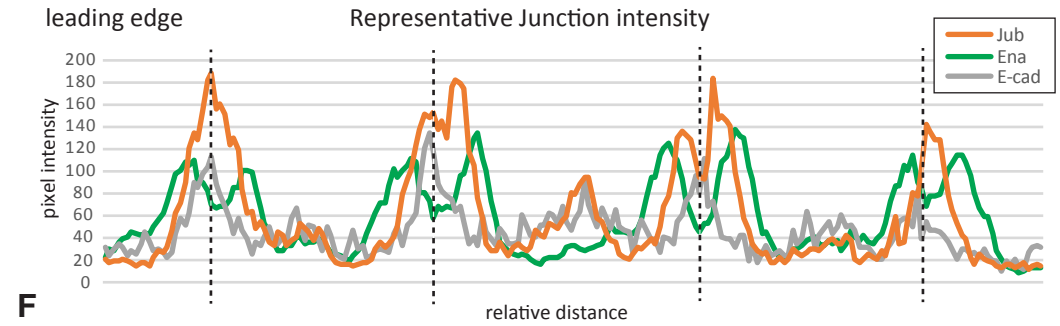

**Figure S1. Jub localization at different stages of development**

A) Localization of Jub:GFP (green/white) in posterior mid-gut invagination, compared to DNA (blue) and Armadillo (Arm, ß-catenin, red/white), B) Jub:GFP (green) and E-cad (red) in dorsal epidermis and leading edge cells during dorsal closure. C) Jub:GFP (green) and E-cad (red) in dorsal epidermis and leading edge cells during dorsal closure in an embryo expressing activated-myosin (UAS-Sqh.EE) under da-Gal4 control. Junctional localization of Jub:GFP is increased, e.g. compare cell labelled by asterisk in B and C. Arrows point to some sites with elevated Jub. D) Wing disc expressing Jub:GFP (green/white) stained for expression of Wg (red) and E-cad (blue/white). E) Left side: Line scan of signal intensity for Jub, Vinc and E-cad along a single junction between wing disc cells (as in Fig. 2A). Right side: Average intensity along wing disc junctions, normalized to the mean junction intensity, and plotted as percent junction length, for Jub (n=42), Vinc (n=25), and E-cad (n=74). E-cad intensity tends to be slightly higher near vertices and lower in the middle of the junction. Bright puncta of Jub and Vinc occur preferentially near vertices, but this preference is not absolute, and the distance of puncta from vertices varies. This is reflected in a slight relative increase in Jub and Vinc around 10-20 and 80-90 percent junction length. Kolmogorov-Smirnov tests of the significance of the difference between distributions identifies a difference between Vinc and E-cad, and between Jub and E-cad, but not between Vinc and Jub. ns, $P>0.05$, * $P\leq0.05$, ** $P\leq0.01$. F) Line scan of signal intensity for Jub, Ena and E-cad along the leading edge (as in Fig. 2C). Dashed lines indicate approximate locations of junctions between dorsal leading edge cells.

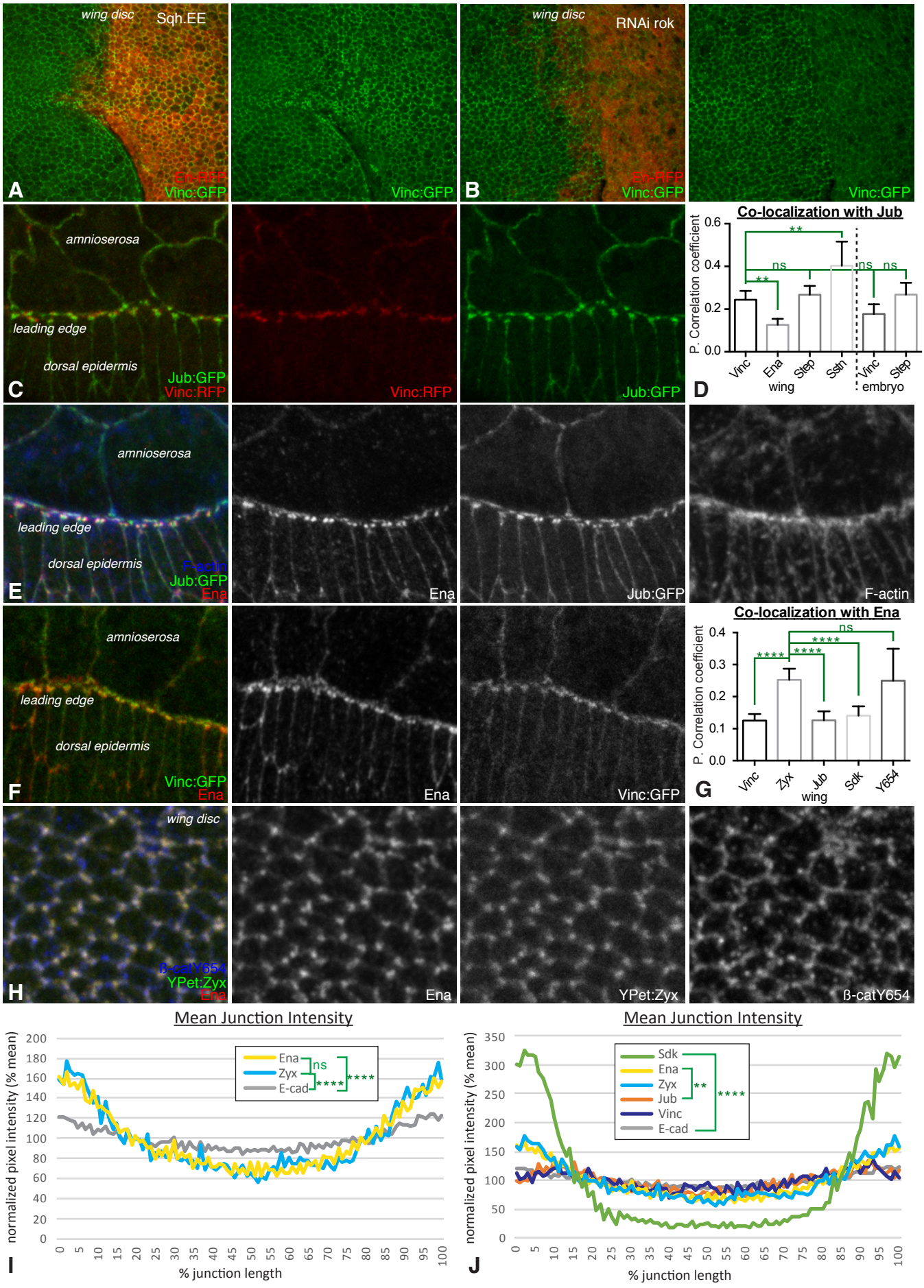


Journal of Cell Science • Supplementary information

**Figure S2. Localization of AJ complex proteins**

A,B) Wing discs expressing Vinc:GFP and in posterior cells under en-Gal4 control UAS-RFP (red) and (A) UAS-Sqh.EE or (B) UAS-RNAi-rok. C,E,F) Leading edge cells during dorsal closure, comparing expression of (C) Vinc:RFP and Jub:GFP, (E) Ena (red/white), Jub:GFP (green/white) and F-actin (blue/white), (F) Ena (red/white) and Vinc:GFP (green/white). D,G) Quantitation of Pearson's co-localization coefficient between Jub and the indicated proteins (D) and between Ena and the indicated proteins (G). For Jub (D), we compare the extent of co-localization between Jub and Vinc in wing discs with the other proteins indicated, only for Ena and Sstn is the extent of co-localization significantly different. For Ena (G), we compare the extent of co-localization with Zyx, which significantly differs from co-localization with Vinc, Jub, and Sdk, but not Y654. H) Wing disc cells expressing UAS-YPet:Zyx under da-Gal4 and act-Gal4 control, stained for Ena (red/white) and pY654-ß-cat. I,J) Average intensities along wing disc junctions, normalized to the mean junction intensity, and plotted as percent junction length, for Ena (n=49), Zyx (n=16) and E-cad (n=74) (I), or Ena, Zyx, E-cad, Jub (n=42), Vinc (n=25), and Sdk (n=17) (J). Distinct plots are provided with differences in scaling, as Sdk is much more tightly localized along junctions as compared to other proteins. A Kolmogorov-Smirnov tests of the significance of the difference between distributions identifies differences between Ena and E-cad, between Zyx and E-cad, between Ena and Jub, and between Sdk and E-cad, but not between Ena and Zyx. ns, $P>0.05$, ** $P\leq0.01$, **** $P\leq0.0001$.

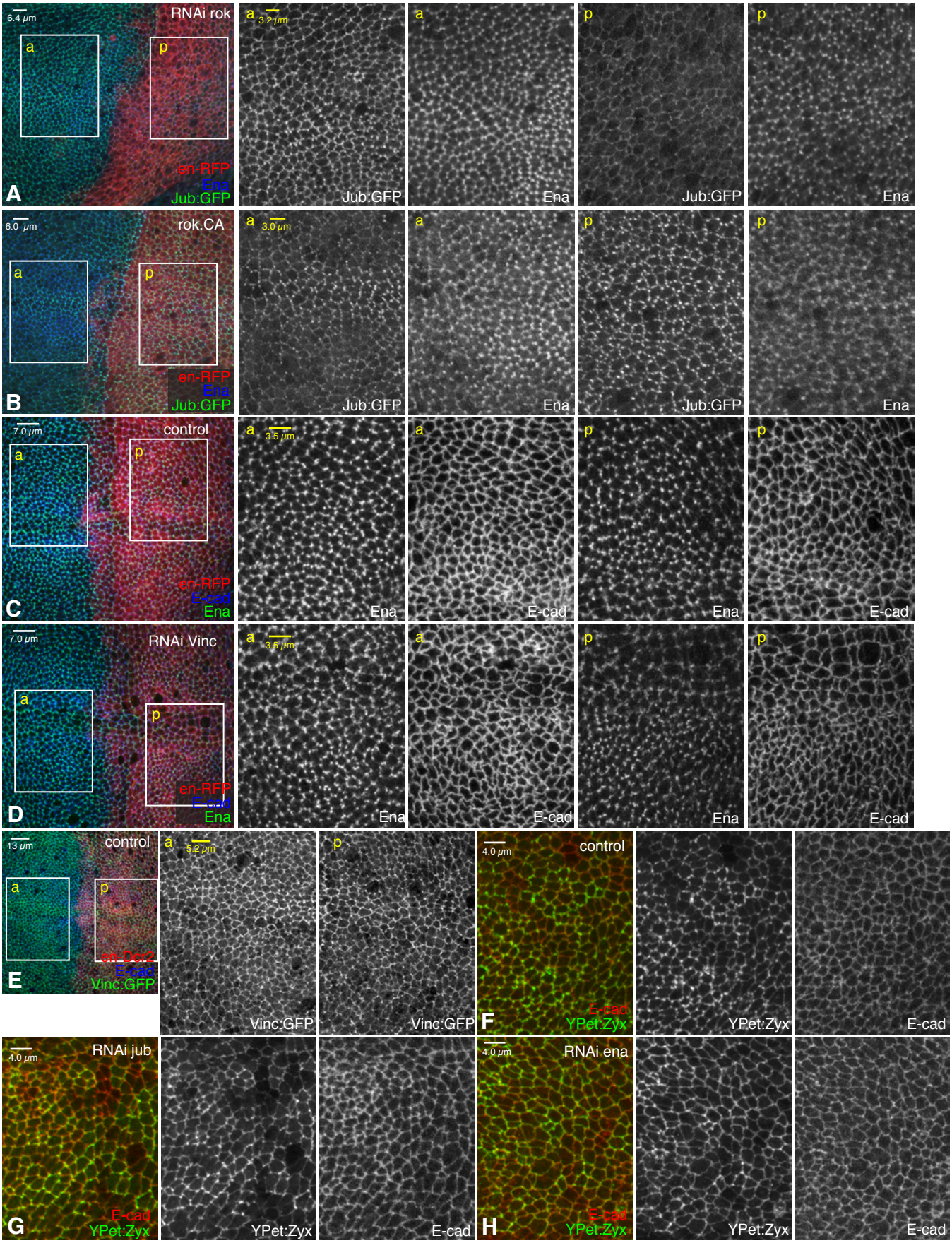
6.4 μm
RNAi rok
a
p
en-RFP
Ena
Jub:GFP
A
a
3.2 μm
Jub:GFP
a
Ena
p
Jub:GFP
p
Ena
6.0 μm
rok.CA
a
p
en-RFP
Ena
Jub:GFP
B
a
3.0 μm
Jub:GFP
a
Ena
p
Jub:GFP
p
Ena
7.0 μm
control
a
p
en-RFP
E-cad
Ena
C
a
3.5 μm
Ena
a
E-cad
p
Ena
p
E-cad
7.0 μm
RNAi Vinc
a
p
en-RFP
E-cad
Ena
D
a
3.5 μm
Ena
a
E-cad
p
Ena
p
E-cad
13 μm
control
a
p
en-Dcr2
E-cad
Vinc:GFP
E
a
5.2 μm
Vinc:GFP
p
Vinc:GFP
4.0 μm
control
E-cad
YPet:Zyx
F
YPet:Zyx
E-cad
4.0 μm
RNAi jub
E-cad
YPet:Zyx
G
YPet:Zyx
E-cad
4.0 μm
RNAi ena
E-cad
YPet:Zyx
H
YPet:Zyx
E-cad

**Figure S3. Influence of tension on Jub and Ena, and independent junctional localization of Ena and Zyx**

Wing imaginal discs in which UAS transgenes were expressed in posterior cells (red) under *en-Gal4* control to assess potential requirements for localization of AJ complex proteins. In A-E, panels to the right show higher magnification images of the anterior (a) or posterior (p) boxes. A) RNAi of rok reduces Jub (green/white) junctional localization, but not Ena (blue/white). B) Activation of Rok (UAS-rok.CA) increases Jub (green/white) junctional localization, but not Ena (blue/white). C) Control wing disc stained for Ena (green/white) and E-cad (blue/white). D) RNAi of Vinc does not affect Ena (green/white) localization. E) Control wing disc expressing Vinc:GFP (green/white) and stained for E-cad (blue/white). F-H) Posterior region of wing discs expressing UAS-YPet:Zyx (green) and (F) control, , (G) UAS-RNAi-jub, (H) UAS-RNAi-ena stained for E-cad (red).

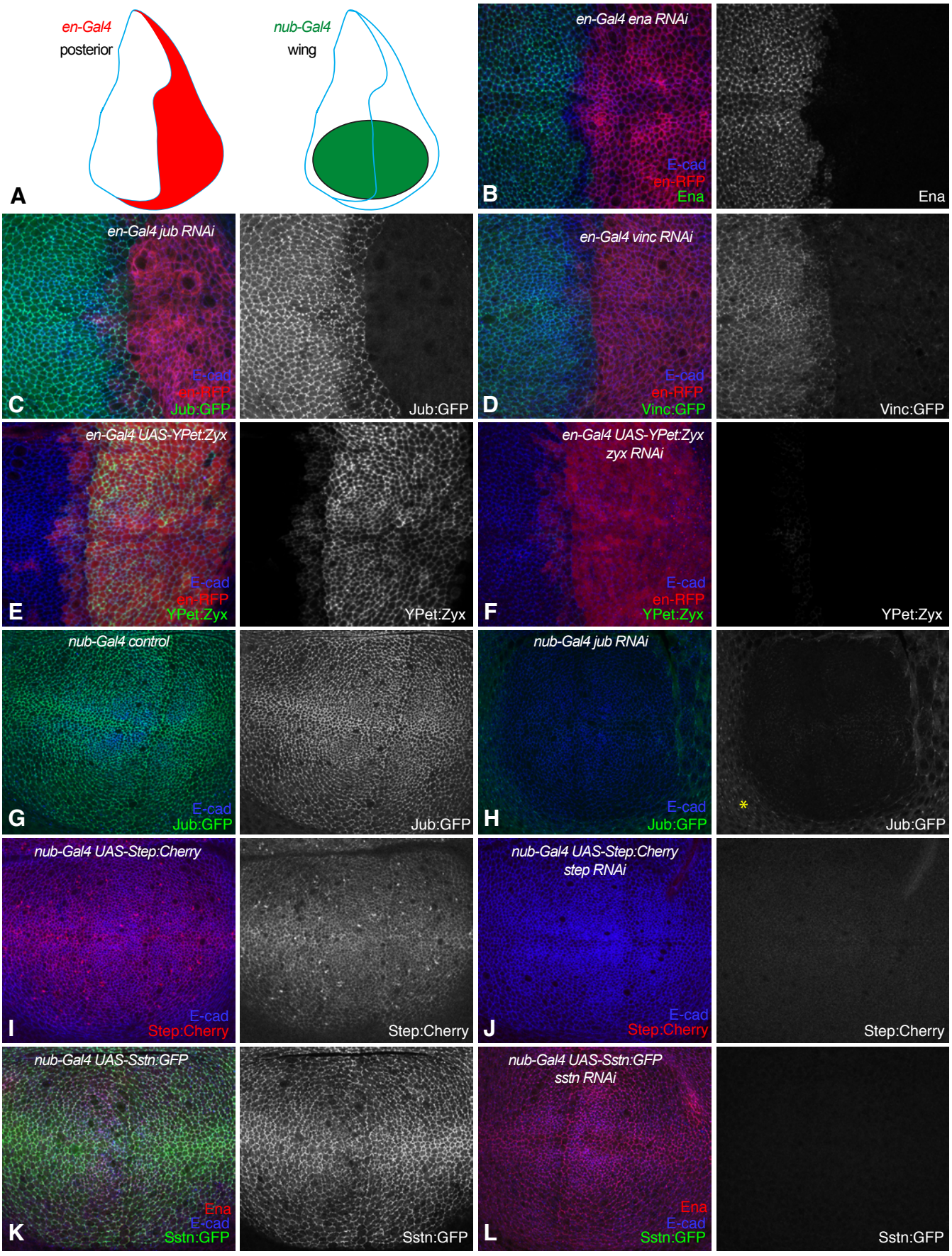

**Figure S4. Effectiveness of RNAi**

A) Schematics illustrating approximate expression domains of en-Gal4 and nub-Gal4 within the wing imaginal disc. B-F) Confocal images of wing imaginal discs expressing UAS transgenes in P cells under en-Gal4 control, stained for E-cad (blue), and: B) UAS-RNAi ena and stained for Ena (green/white). C) Jub:GFP (green/white) and UAS-RNAi jub. D) Vinc:GFP (green/white) and UAS-RNAi Vinc. E) UAS-YPet:Zyx (green/white). F) UAS-YPet:Zyx (green/white) and UAS-RNAi Zyx. G-L) Confocal images of wing imaginal discs expressing UAS transgenes in wing cells under nub-Gal4 control, stained for E-cad (blue), and: G) Jub:GFP (green/white). H) Jub:GFP (green/white) and UAS-RNAi jub. Proximal signal (asterisk) comes from outside the nub-Gal4 expression domain, which is reduced in size due to *jub* RNAi. I) UAS-Step:Cherry (red/white). J) UAS-Step:Cherry (red/white) and UAS-RNAi step. K) UAS-Sstn:GFP (green/white). L) UAS-Sstn:GFP (green/white) and UAS-RNAi sstn.

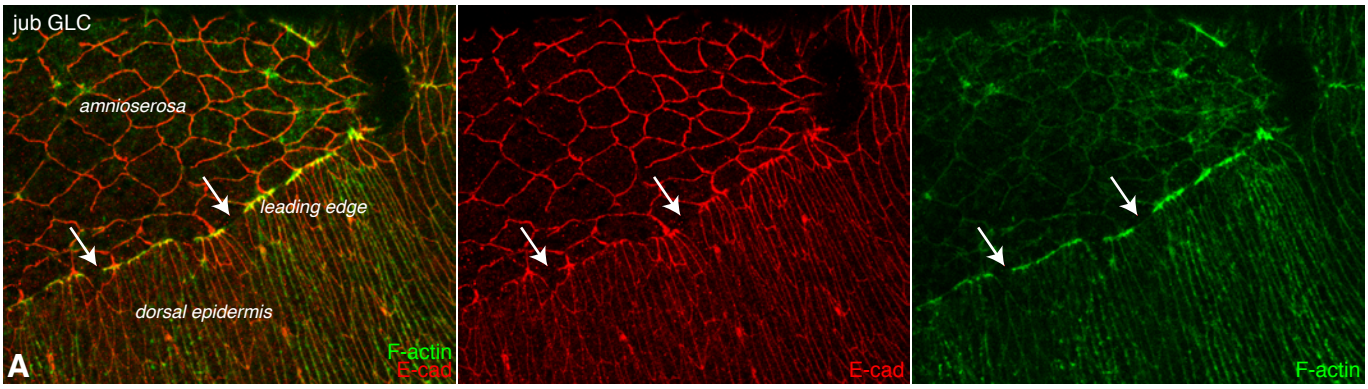


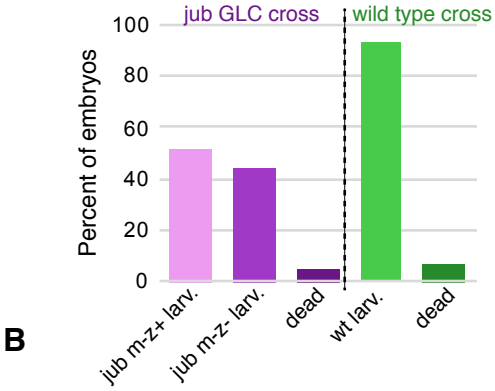


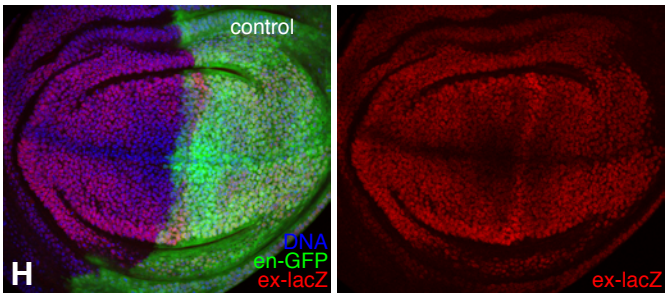


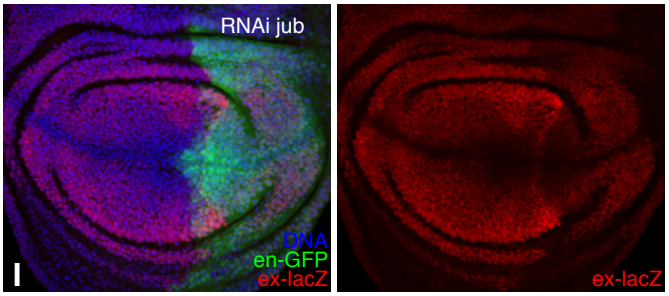


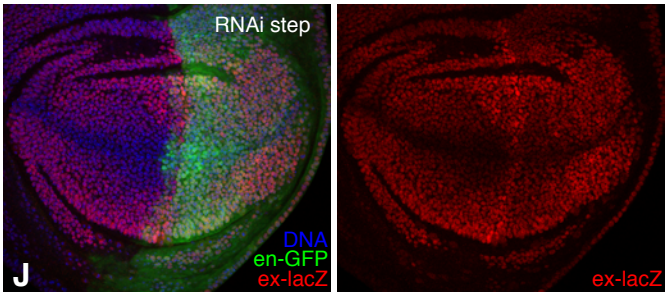


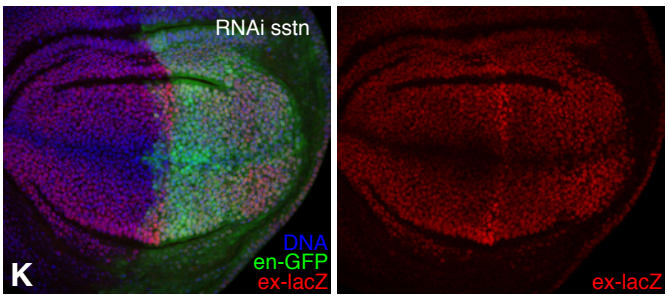


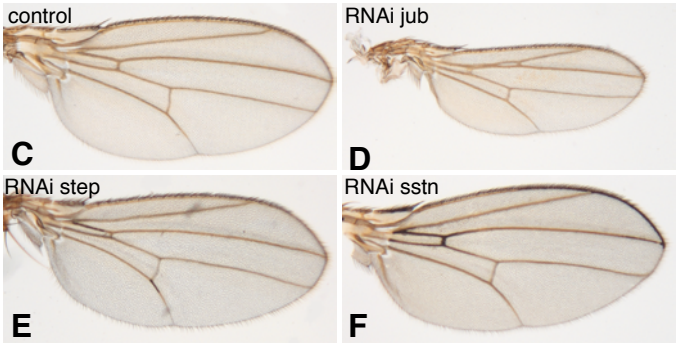


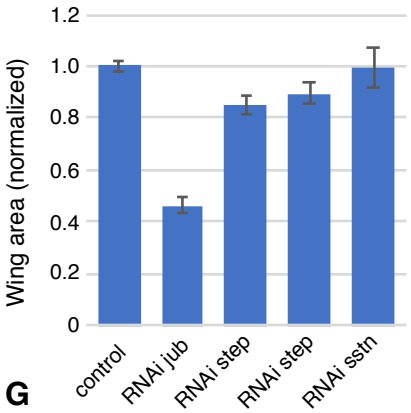

**Figure S5. Phenotypes of *jub* and *step***

A) Example of *jub* embryo with gaps (highlighted by arrows) in the leading edge cable revealed by staining for E-cad and F-actin. B) Quantitation of embryonic viability in a cross of females with *jub* germline clones to FM7, Dfd-YFP males (magenta) and in wild-type (Oregon-R) control (green). The germline clone cross generates *jub*$^{-}$ males (m-z-, n=169)*, and jub*$^{-}$ */ FM7 Dfd-YFP* females (m-z+, n=197). The Dfd-YFP marker can be reliably scored in live embryos and larvae, but not in dead embryos (n=17); as an upper limit, if all dead embryos are m-z- then 9% (17/186) of progeny are embryonic lethal. In the control 7% (14/197) of offspring died during embryogenesis. C-F) Adult wings from flies expressing nub-Gal4 and (C) control, (D) UAS-RNAi-jub, (E) UAS-RNAi-step, (F) UAS-RNAi-sstn. G) Histogram showing wing size, normalized to control wings, in flies expressing the indicated UAS-RNAi lines. N=10 (control, jub, step HMS), 13 (step vdrc), or 14 (sstn). error bars indicate s.d. H-K) Wing discs expressing RNAi lines in posterior cells (green) under en-Gal4 control, and stained for ex-lacZ (red) and DNA(blue), and expressing, H) control, I) UAS-RNAi-jub, J) UAS-RNAi-step, K) UAS-RNAi-sstn.

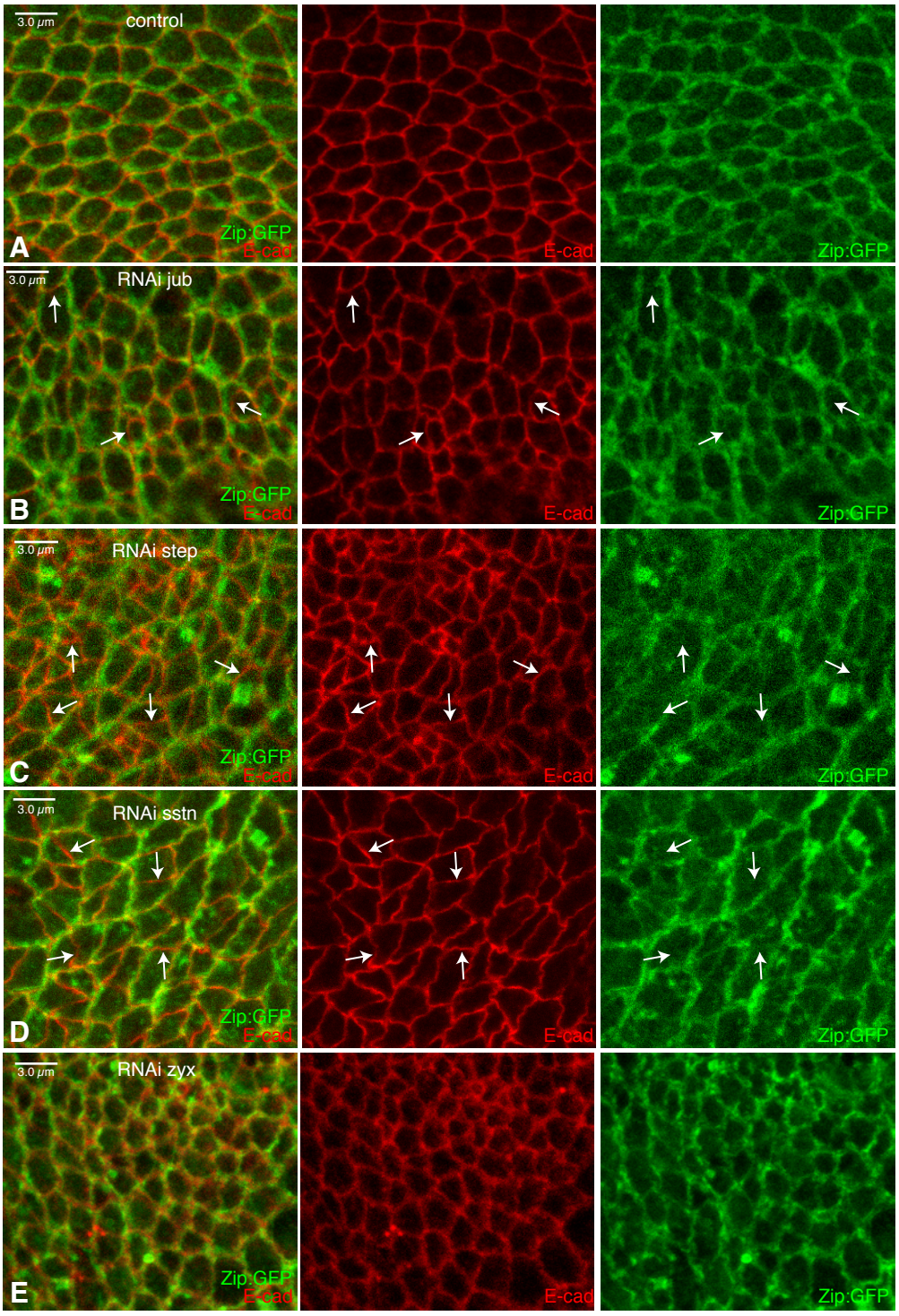


**Figure S6. Influence of *jub*, *step, sstn* and *zyx* on wing disc epithelia**

Wing disc cells expressing RNAi lines under *en-Gal4* control, stained for E-cad (red) and also expressing Zip:GFP (green). A) control. B) UAS-RNAi-jub. C) UAS-RNAi-step. D) UAS-RNAi-sstn. E) UAS-RNAi-Zyx. Arrows highlight examples of AJ with little or no associated myosin (Zip:GFP).

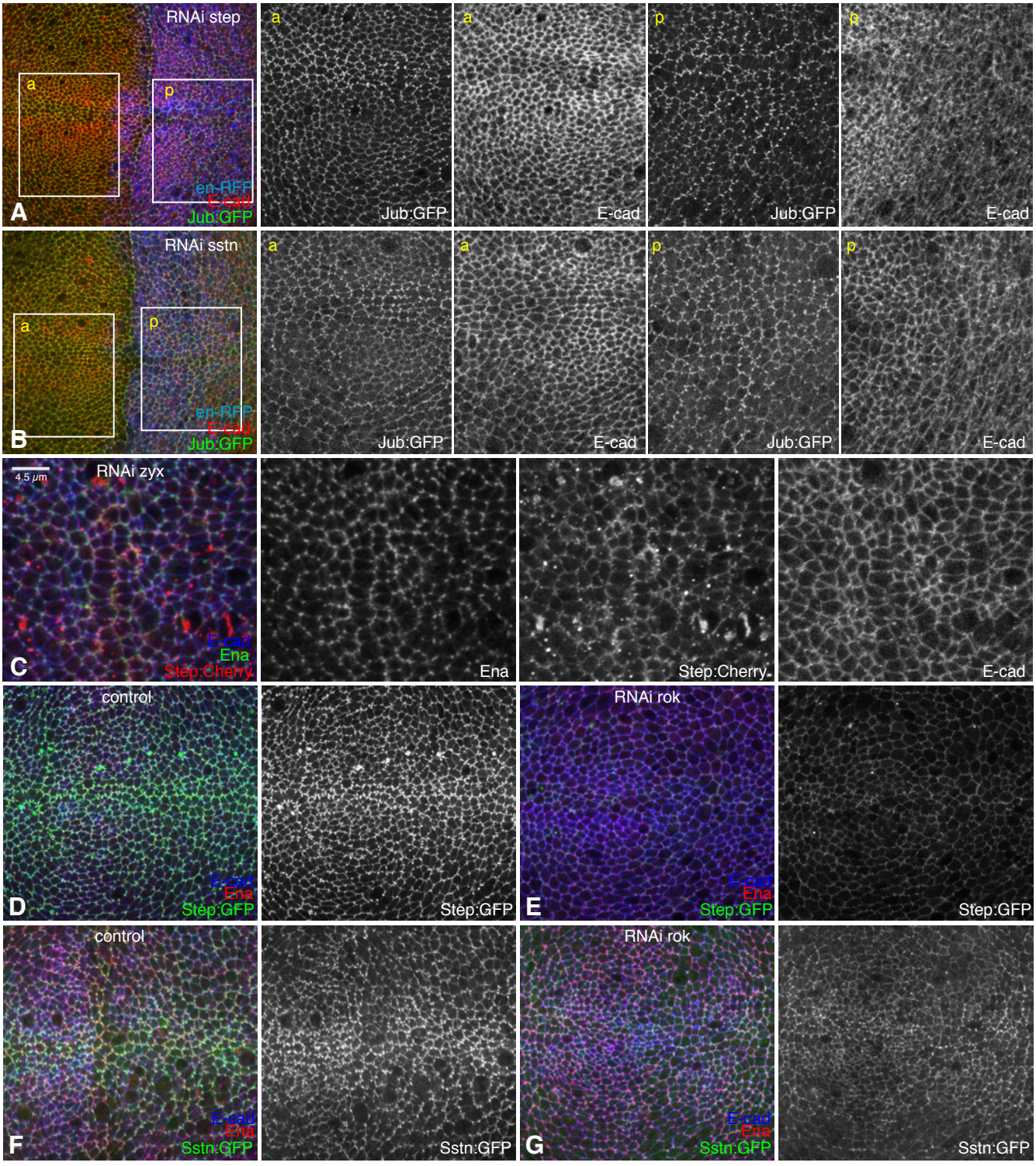
RNAi step
a
p
en-RFP
E-cad
Jub:GFP
A
a
Jub:GFP
a
E-cad
p
Jub:GFP
p
E-cad
RNAi sstn
a
p
en-RFP
E-cad
Jub:GFP
B
a
Jub:GFP
a
E-cad
p
Jub:GFP
p
E-cad
4.5 μm
RNAi zyx
E-cad
Ena
Step:Cherry
C
Ena
Step:Cherry
E-cad
control
E-cad
Ena
Step:GFP
D
Step:GFP
RNAi rok
E-cad
Ena
Step:GFP
E
Step:GFP
control
E-cad
Ena
Sstn:GFP
F
Sstn:GFP
RNAi rok
E-cad
Ena
Sstn:GFP
G
Sstn:GFP

**Figure S7. Regulation of Step and Sstn localization in wing discs, and lack of influence of Step and Sstn on Jub**

Wing discs expressing UAS-RNAi lines either in posterior cells (marked by UAS-RFP, blue) under *en-Gal4* control (A,B), or in all wing cells under *nub-Gal4* control (C-G), stained for expression of E-cad (red/white/blue). A) RNAi-*step* does not lead to loss of Jub (green/white). B) RNAi-*sstn* does not lead to loss of Jub (green/white). C) UAS-RNAi-Zyx does not remove UAS-Step:Cherry (red/white) from cell membranes. D) Control expressing UAS-Step:GFP. E) UAS-RNAi-rok results in a decrease in UAS-Step:GFP levels. F) Control expressing UAS-Sstn:GFP. G) UAS-RNAi-rok slightly reduces UAS-Sstn:GFP. Identical imaging conditions were used for (D) and (E), and for (F) and (G) and thus they are directly comparable.

## Supplemental Movies

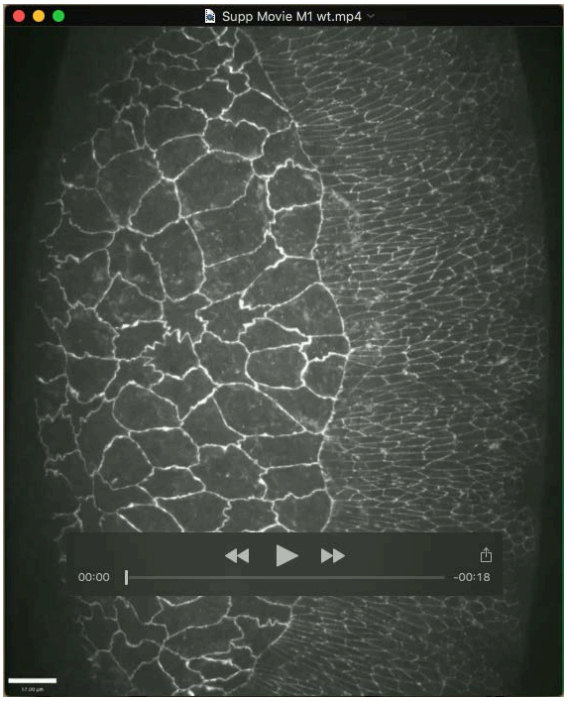


**Movie 1. Dorsal closure in a *wild-type* embryo.** Dorsal epidermal cells of a wild-type embryo, outlined by E-cad:GFP. Time is at upper right, and a scale bar is at lower left.

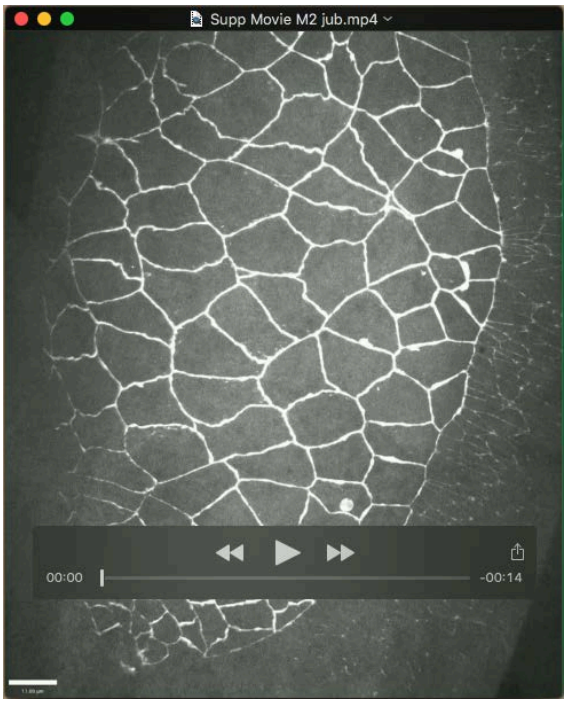


**Movie 2. Dorsal closure in a *jub* embryo.** Dorsal epidermal cells of a *jub* germ line clone embryo, outlined by E-cad:GFP. Time is at upper right, and a scale bar is at lower left.